

## Supplementary information

### Highly dispersed Pt nanoclusters supported on zeolite-templated carbon for oxygen reduction reaction

Raj Kumar Bera,<sup>\*a</sup> Hongjun Park,<sup>a,b</sup> Seung Hyeon Ko<sup>a</sup> and Ryong Ryoo<sup>\*a,b</sup>

<sup>a</sup>. Center for Nanomaterials and Chemical Reactions, Institute for Basic Science (IBS), Daejeon, 34141, Republic of Korea

E-mail: [chemsraj@ibs.re.kr](mailto:chemsraj@ibs.re.kr)

<sup>b</sup>. Department of Chemistry, Korea Advanced Institute of Science and Technology (KAIST), Daejeon, 34141, Republic of Korea

E-mail: [rryoo@kaist.ac.kr](mailto:rryoo@kaist.ac.kr)

### Experimental Section

#### Synthesis of Pt nanocluster supported on zeolite-templated carbon (PtNC/ZTC)

**electrocatalyst:** The ZTC was synthesized using beta zeolite (Tosoh) as a template and ethylene as a carbon precursor, following the same procedure as previously reported.<sup>1</sup> In a typical synthesis of PtNC/ZTC, an adequate amount of H<sub>2</sub>PtCl<sub>6</sub>·6H<sub>2</sub>O (Sigma-Aldrich) dissolved in a 1:4 water-ethanol mixture (in volume ratio) was loaded into 80 mg of ZTC support by the incipient wetness impregnation method and dried at 60 °C. A catalyst ink was prepared with 10 mg of the PtCl<sub>6</sub><sup>2-</sup>-impregnated ZTC, 0.2 mL of water, 0.05 mL of 5 wt% Nafion (Sigma-Aldrich), and 0.75 mL of ethanol after sonication for 30 min. The working electrode was prepared by dropping 8 μL of the prepared ink on a glassy carbon electrode (*d* = 5 mm) and dried at room temperature. After electrode preparation, a potential of -0.2 V (vs Ag/AgCl, 3M KCl) was applied, followed by potential cycling between 0.15 to -1 V (vs Ag/AgCl, 3M KCl) in an N<sub>2</sub>-purged 0.1 M KOH electrolyte until a stabilized cyclic voltammogram was obtained. The resultant PtNC/ZTC electrode was then washed with water and applied to the oxygen reduction reaction (ORR) in fresh 0.1 M KOH or HClO<sub>4</sub> electrolyte.

**Characterization:** For the characterization, PtNC/ZTC was collected from the electrode surface by sonication in ethanol. Scanning transmission electron microscope (STEM) images were taken with a Titan cubed G2 60-300 instrument operated at an acceleration voltage of 300 kV and equipped with a spherical aberration corrector. Transmission electron microscope (TEM) images were acquired with an FEI Titan ETEM G2 microscope operated at 300 kV. For Thermogravimetric analysis (TGA), X-ray powder diffraction (XRD), and Brunauer–Emmett–Teller (BET) analyses, PtNC/ZTC was prepared on a glassy carbon plate with an area of 25 × 25 mm<sup>2</sup>. TGA was conducted using a TA Instruments TGA Q50 analyzer. For TGA

measurement, the sample was heated to 800 °C at a ramping rate of 5 °C min<sup>-1</sup>, under a mixture of N<sub>2</sub> gas flow of 40 cm<sup>3</sup> min<sup>-1</sup> and airflow of 60 cm<sup>3</sup> min<sup>-1</sup>. XRD patterns were collected on a Rigaku SmartLab diffractometer with Cu K $\alpha$  radiation (30 kV, 40 mA). Ar adsorption-desorption isotherms were obtained with a Quantachrome Autosorb-iQ gas adsorption analyzer. According to BET theory, the specific surface area was determined in the region of relative pressure between 0.05 and 0.15. XPS was performed using a Thermo Scientific K-alpha spectrometer with monochromatized Al K $\alpha$  radiation.

**Electrochemical measurements:** All electrochemical measurements were performed with an Autolab PGSTAT30 workstation at 25 °C. The potential values, measured against an Ag/AgCl (3 M KCl) electrode, were converted to potential versus reversible hydrogen electrode (RHE) using the equation:  $E_{\text{RHE}} = E_{\text{Ag/AgCl}} + 0.210 + 0.059 \text{ pH}$ . Commercial 37.4 wt% Pt/C-TKK (Tanaka Kikinokogyo) was used as a reference material for the ORR. A 0.1 M KOH or HClO<sub>4</sub> aqueous solution saturated with O<sub>2</sub> gas was used as the electrolyte for ORR. The LSV curve was corrected by compensating the iR drop and subtracting the nonfaradaic capacitive current, which was obtained by taking the LSV curve under an N<sub>2</sub>-saturated environment. The Koutecky–Levich (K-L) plots were derived at different potentials from the LSV curves obtained at various rotation speeds. The number of electrons transferred per oxygen molecule ( $n$ ) was determined from the slope ( $B$ ) of the K-L plot based on the K-L equation,  $1/j = 1/j_K + 1/B\omega^{1/2}$   $B = 0.2nF(D_0)^{2/3}C_0 \nu^{-1/6}$ , where  $j$  is the measured current density,  $j_K$  is the kinetic-limiting current density,  $\omega$  is the electrode rotation rate,  $F$  is the Faraday constant (96 485 C mol<sup>-1</sup>),  $D_0$  is the diffusion coefficient of O<sub>2</sub> in 0.1 M KOH (1.9 x 10<sup>-5</sup> cm<sup>2</sup> s<sup>-1</sup>),  $C_0$  is the bulk concentration of O<sub>2</sub> (1.2×10<sup>-6</sup> mol cm<sup>-3</sup>), and  $\nu$  is the kinetic viscosity (0.01 cm<sup>2</sup> s<sup>-1</sup>). The number electron was also calculated from rotating ring-disc electrode (RRDE) curve using  $4 \times i_d / (i_d + i_r / N)$  equation and the percentage of peroxide generated during ORR were calculated using  $200 \times i_r / N(i_d + i_r / N)$  equation, where  $i_d$  is the disc current,  $i_r$  is the ring current, and  $N$  is the geometric factor of the RRDE known as current collection efficiency of the Pt ring (0.249). The mass activity was determined using the mass transport corrected kinetic current ( $i_k$ ), which can be derived from the experimental data using  $(1/i_k = 1/i - 1/i_L)$ , where  $i_L$  is the diffusion limiting current and  $i$  is the measured current at 0.8 V vs RHE at kinetic-diffusion control region.

## Reference

- 1 H. Park, S. K. Terhorst, R. K. Bera and R. Ryoo, Carbon, 2019, 155, 570.

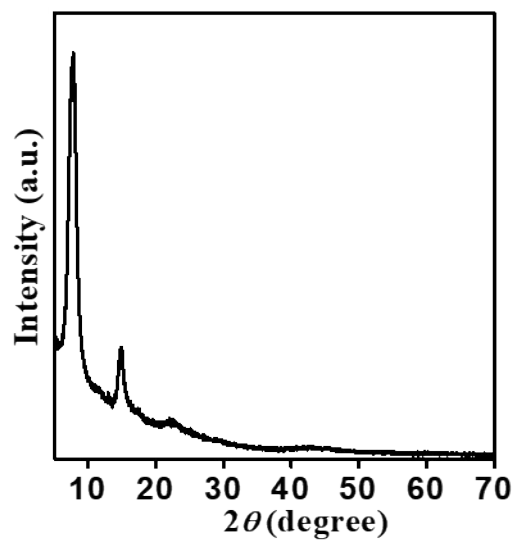


**Fig. S1** X-ray powder diffraction pattern of zeolite-templated carbon (ZTC) used in this work, showing an ordered microporous structure.

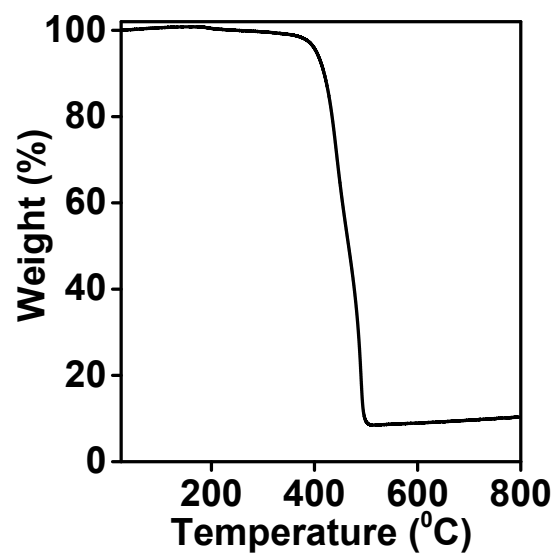


**Fig. S2** Thermogravimetric analysis profile of Pt nanocluster loaded on ZTC (PtNC/ZTC).

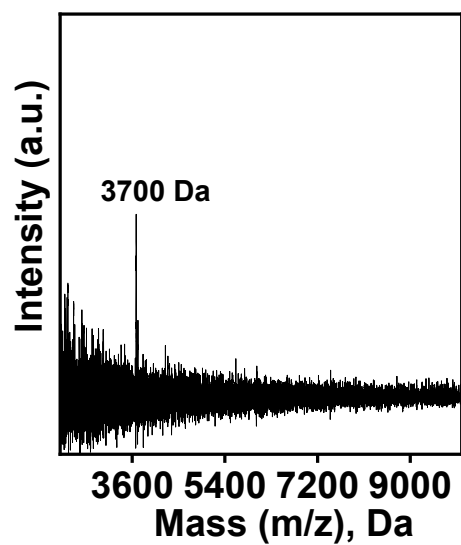


**Fig. S3** Matrix-assisted laser desorption/ionization time-of-flight mass spectrum of PtNC/ZTC showing a predominant peak centered at  $\sim 3,700$  Da corresponds to the  $\text{Pt}_{19}$  cluster.

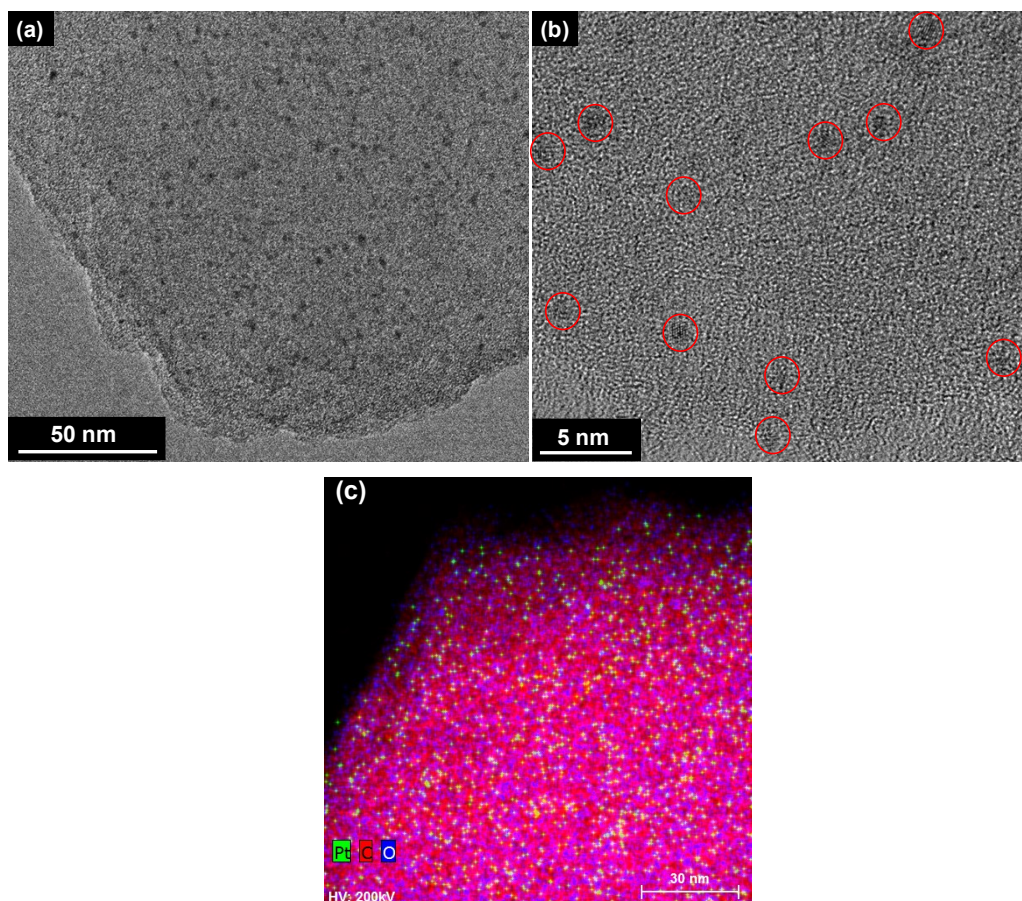


**Fig. S4** The transmission electron microscope image of PtNC/ZTC at (a) a low magnification showing the dispersion of PtNC and (b) a high magnification showing the clusters with an average size of  $\sim 0.9$  nm (red circles indicating the location of PtNC in the image). (c) Energy dispersive X-ray spectrometer mapping image of PtNC/ZTC clearly showing the homogenous dispersion of Pt (green spot).

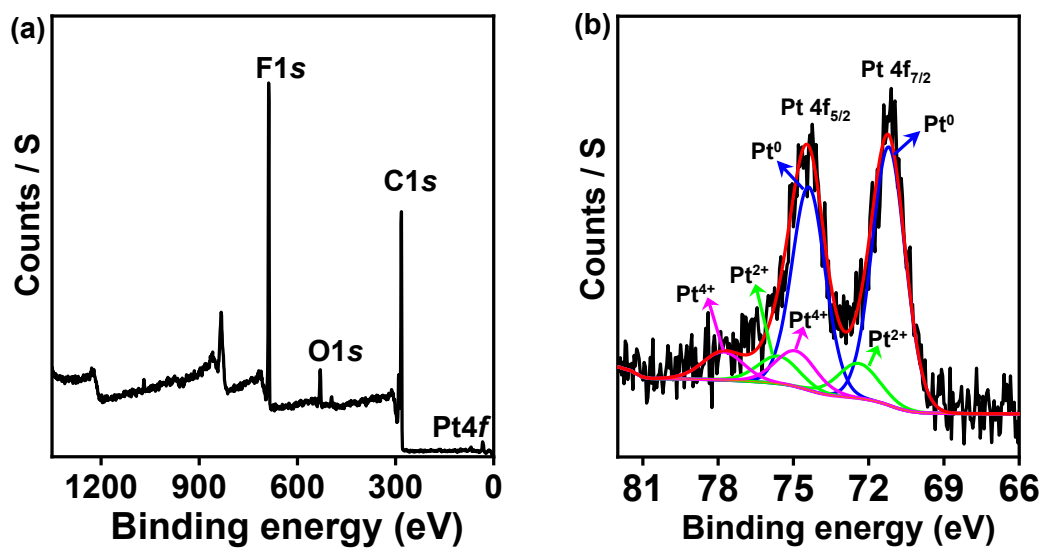


**Fig. S5** The X-ray photoelectron spectroscopy (XPS) of PtNC/ZTC. (a) elemental survey and (b) deconvoluted Pt4f XPS spectra.

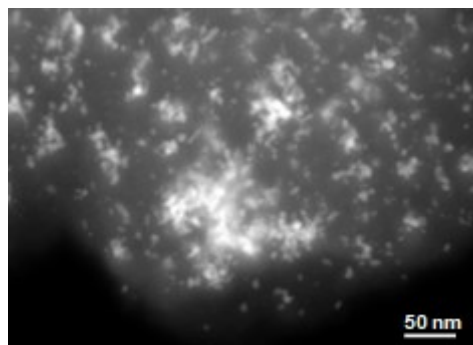


**Fig. S6** High-angle annular dark-field scanning transmission electron microscope (HAADF STEM) image of PtNP/ZTC prepared by conventional incipient wetness impregnation and subsequent H<sub>2</sub>-reduction at high temperature.



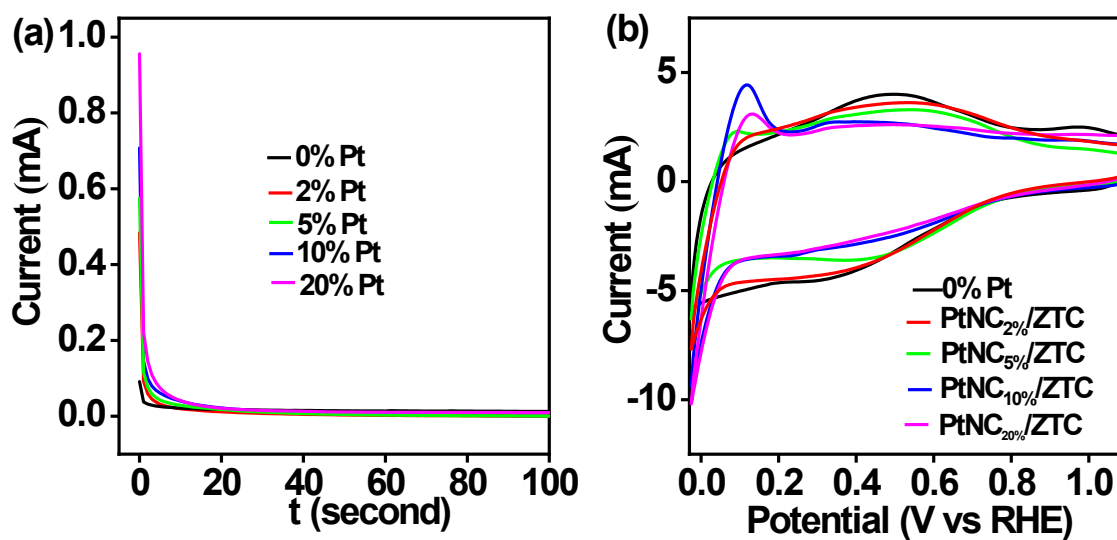


**Fig. S7** Preparation of PtNC/ZTC with various Pt loading of 2-20 wt%. (a) Chronoamperometric responses with different loading of Pt in ZTC and (b) cyclic voltammogram (CV) of PtNC/ZTC with different loading of Pt.

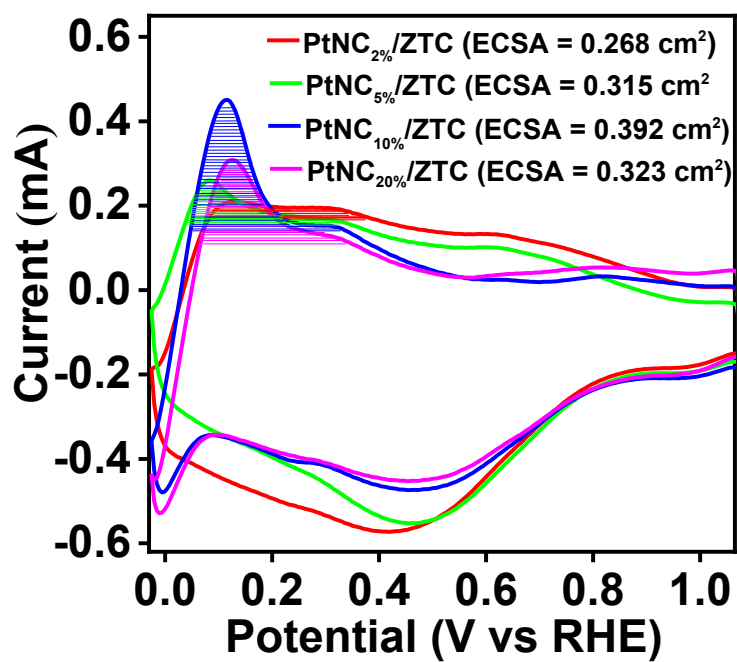


**Fig. S8** Double-layer charge corrected CV of PtNC/ZTC. The shaded area (H desorption region) in the figure was used for the determination of the electrochemically active surface area (ECSA).

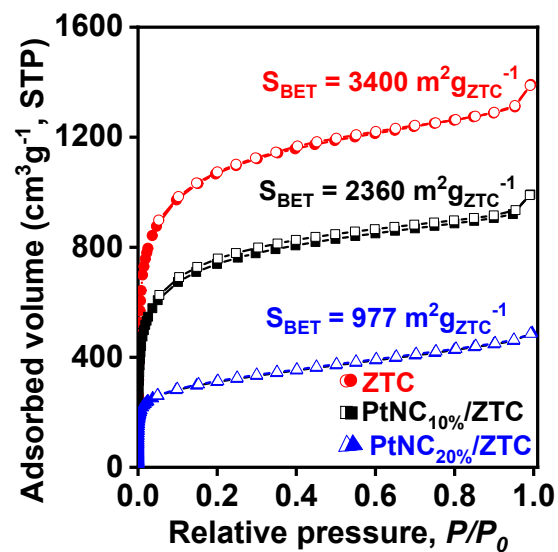


**Fig. S9** Ar adsorption-desorption isotherms of ZTC and PtNC/ZTC with 10 and 20 wt% loading of Pt, revealing 72 and 59 % decrease in surface area compared to that of pristine ZTC and PtNC<sub>10%</sub>/ZTC, respectively.

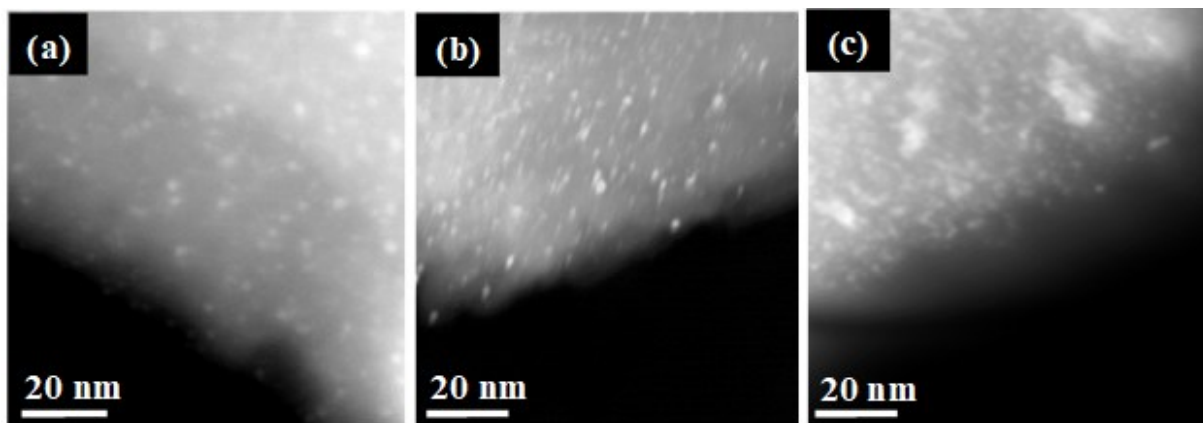


**Fig. S10** HAADF-STEM images of PtNC/ZTC with different loading of Pt; (a) 2 wt%, (b) 5 wt%, and (c) 20 wt%.

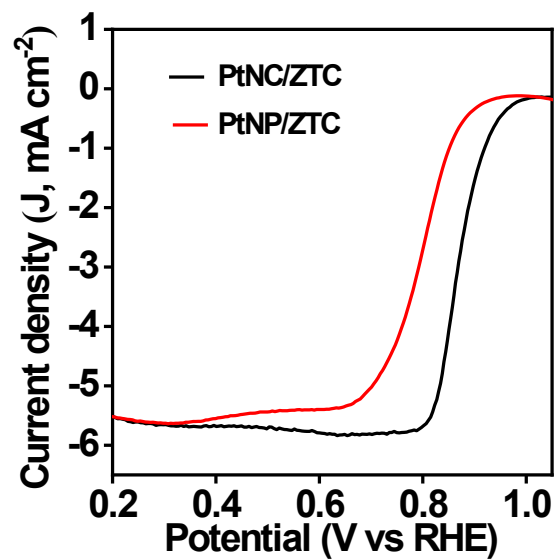


**Fig. S11** Rotating disc electrode (RDE) oxygen reduction reaction (ORR) polarization curves obtained at 1,600 rpm of PtNP/ZTC prepared by the conventional incipient wetness impregnation and subsequent H<sub>2</sub>-reduction at high-temperature method and compared with PtNC/ZTC prepared by electrochemical method.

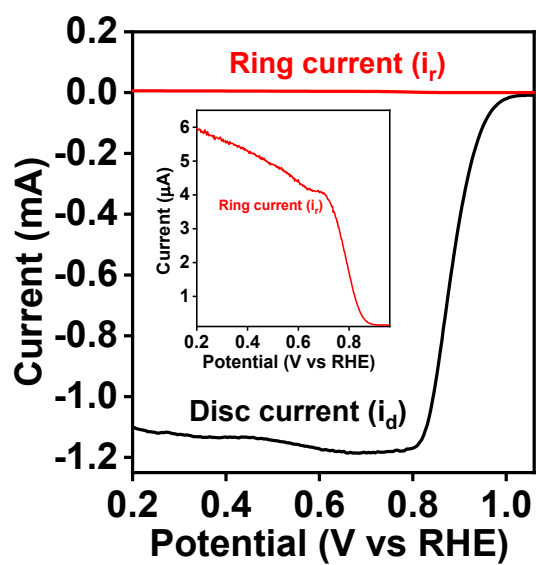


**Fig. S12** RRDE polarization curves PtNC/ZTC at 1,600 rpm in an O<sub>2</sub>-saturated 0.1 M KOH. Inset shows the enlarged ring current.

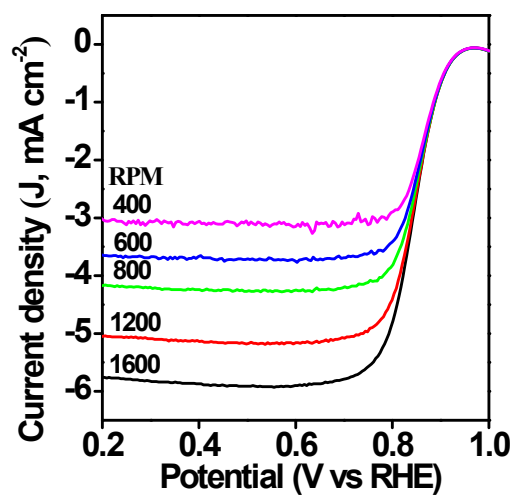


**Fig. S13** RDE ORR polarization curves of PtNC/ZTC at different rotation speeds, in 0.1 M HClO<sub>4</sub>.

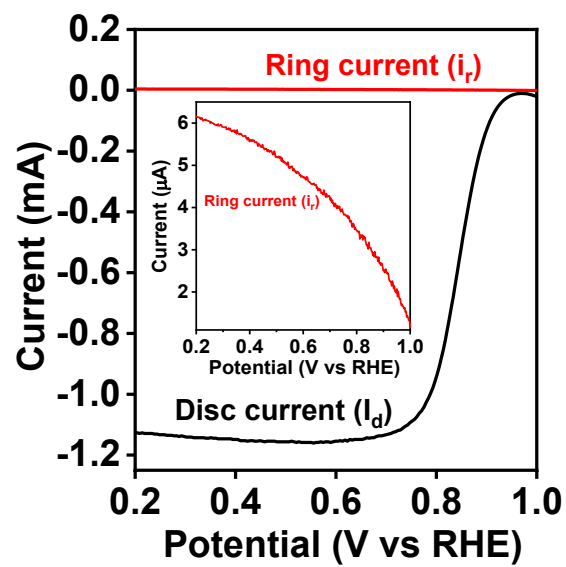


**Fig. S14** RRDE polarization curves of PtNC/ZTC at 1,600 rpm in 0.1 M  $\text{HClO}_4$ . Inset shows the enlarged ring current.



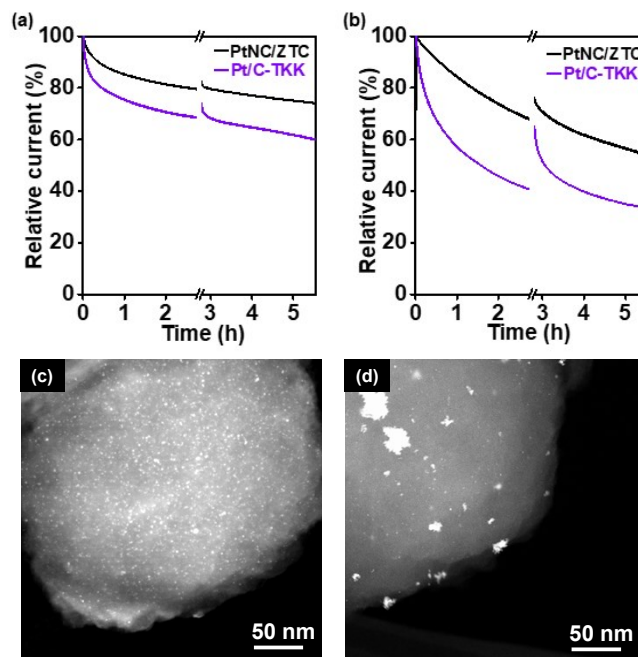


**Fig. S15** Chronoamperometric responses of PtNC/ZTC and Pt/C-TKK at 1,600 rpm in the (a) alkaline media at half-wave potential and (b) acidic media at 0.7 V. HAADF-STEM images of PtNC/ZTC after 5.5 h of ORR operation in (c) alkaline and (d) acidic media.